

Lawrence Berkeley National Laboratory

Recent Work

Title

An Efficiency-Focused Design of Direct-DC Loads in Buildings

Permalink

<https://escholarship.org/uc/item/12q8m3p0>

Authors

Gerber, Daniel

Liou, Richard

Brown, Richard

Publication Date

2022-08-20

Peer reviewed

An Efficiency-Focused Design of Direct-DC Loads in Buildings

Daniel L Gerber
Bldg Tech Urban Systems (BTUS)
Lawrence Berkeley Labs
Berkeley, CA, USA
dgerb@lbl.gov

Richard Liou
Elec Eng Comp Sci (EECS)
University of California Berkeley
Berkeley, CA, USA
rliou92@lbl.gov

Richard Brown
Bldg Tech Urban Systems (BTUS)
Lawrence Berkeley Labs
Berkeley, CA, USA
rebrown@lbl.gov

Abstract—Despite the recent interest in direct current (DC) power distribution in buildings, the market for DC-ready loads remains small. The existing DC loads in various products or research test beds are not always designed to efficiently leverage the benefits of DC. This work addresses a pressing need for a study into the development of efficient DC loads. In particular, it focuses on documenting and demonstrating how to best leverage a DC input to eliminate or improve conversion stages in a load’s power converter. This work identifies how typical building loads can benefit from DC input, including bath fans, refrigerators, task lights, and zone lighting. It then details the development of several prototypes that demonstrate efficiency savings with DC. The most efficient direct-DC loads are explicitly designed for DC from the ground up, rather than from an AC modification.

Keywords—DC distribution, plug loads, direct DC, buildings, variable frequency drive, LED lighting

I. BACKGROUND AND MOTIVATION

A. Motivation for DC Distribution in Buildings

Direct current (DC) power distribution systems have become a recent topic in building energy research as a means of reducing power consumption. In the past, alternating current (AC) was well suited to power the nineteenth and twentieth century loads such as incandescent lamps, resistive heating, and fixed speed motors. However, with the proliferation of electronics, light emitting diode (LED) lighting, and variable frequency drives (VFDs) for motor-driven loads, an increasing fraction of today’s electric loads operate internally on DC. In addition, the recent growth in on-site photovoltaic (PV) generation and battery storage adds even more DC electronics to the building network. DC power distribution for on-site generation, storage, and loads can reduce losses in converting between AC and DC, leading to electricity savings across the board.

The potential electricity savings from DC distribution systems in buildings have been addressed in numerous studies [1]–[10]. For the commercial building sector, the reported savings vary widely from 2% [1] to as much as 19% [2]. Gerber et al. [7] performed a series of highly-detailed simulations, which found low-power load rectifiers to contribute the most loss in AC buildings.

Systems with 380 V DC distribution have been proposed and successfully implemented in data centers with predominantly electronic loads [11]. Commercial buildings have seen

several instances of early adoption for DC distribution systems, primarily in lighting applications [10], [12]. Several other experiments developed DC loads and test beds to evaluate the savings and power quality with DC [9], [10], [13], [14]. Many of these experimental DC loads and test beds exhibit significantly lower savings than those predicted by past analyses and simulations. This work suggests ways in which experimental loads in DC test beds can be improved.

B. Previous Works in DC Modification

Currently, there is a small market for DC plug loads for RV and boating applications [15]. These loads are often compact and designed for 12 V or 24 V DC from the vehicle’s battery. In the next few decades, this market will expand to low-voltage DC solar home systems in developing countries that currently lack universal electrification.

Several previous works have prototyped DC plug loads for newly constructed DC buildings in the residential and commercial sectors. Many of these efforts create prototypes for a variety of DC appliances as a means of performing system or microgrid tests [16]–[20]. Recent research has produced DC prototypes in many end-use categories such as lighting [9], [17]–[21], motor loads [17], [19], [20], [22]–[24], electronics [17]–[20], [25], and induction cooking [18], [26].

Despite the wealth of research on developing DC loads, there are still several important gaps. First, many of the previous works compare AC and DC loads of different technologies. It has been common, for example, to compare a DC variable frequency drive motor appliance to an outdated AC synchronous fixed-speed motor. Second, many of the previous prototypes are not designed to operate at the DC distribution voltages and require DC/DC converters at the input. Such practice neglects the many design optimizations allowed by DC that can benefit efficiency and cost. Finally, most of the previous studies use prototype DC plug loads, but do so as a means of showcasing another research topic such as a DC microgrid demonstration or a new control strategy.

This work aims to improve on previous works by focusing on the optimal development of DC loads. It examines a bathroom fan, refrigerator, LED task lamp, and LED zone lighting rig. These loads are selected to represent the end-use categories of ventilation, refrigeration, and lighting in residential or small commercial buildings. For each load, this

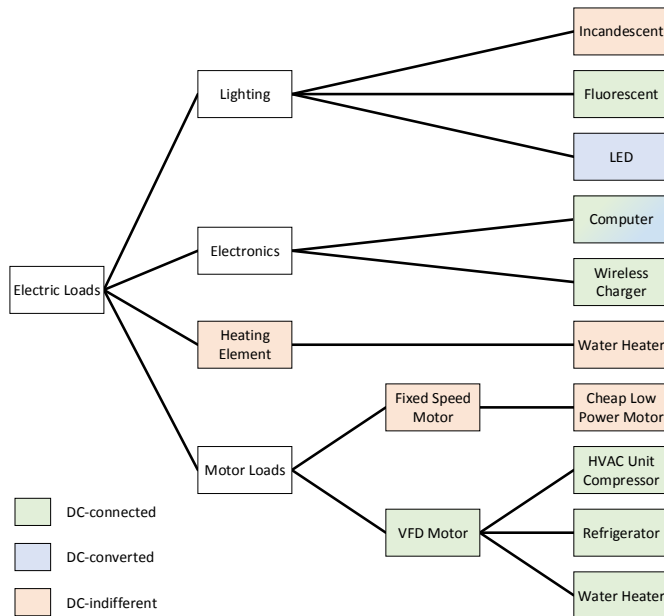


Fig. 1: DC-connected loads have an internal DC stage that can be connected or hardwired to DC distribution. DC-converted loads require an input DC/DC converter, but still benefit from a DC input. DC-indifferent loads do not benefit from a DC input.

work suggests ideas and practices that can be implemented to reap the full benefits of DC.

II. DC LOAD MODIFICATIONS

A. Existing DC Voltage Standards

There are several considerations in selecting the DC distribution voltage. First and foremost is electrical safety, and OSHA standard 1910.303(g)(2)(i) [27] considers voltages below 50 V AC or DC to be touch-safe. Second, higher voltages require more insulation to protect against dielectric breakdown. Finally, low-voltage systems can experience high wire loss and voltage drop. For a device with constant power requirements P_L , the current can be expressed as $I = P_L/V$. Since the wire loss $P_w = I^2 R_w$ decreases quadratically with the wire's voltage, high-power devices are often wired on high-voltage lines.

This work investigates several existing or emerging standards for DC plug voltages:

- USB Type C: 5-20 V, 100 W
- PoE: 48-56 V, 100 W
- EMerge Alliance Data Center Standard: 380 V.

B. Devices that Benefit from DC

Internally DC loads are classified as being direct-DC or native-DC, depending on whether the building distribution is DC or AC, respectively [1]. Direct-DC loads connect to the DC network directly or through a DC/DC converter. Native-DC loads always require a rectifier to interface with the AC distribution.

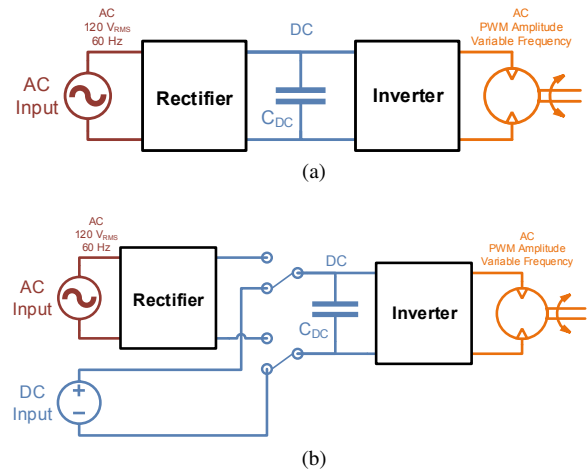


Fig. 2: Block schematic of a VFD motor, as present in the refrigerator and bathroom fan. The inverter is powered from an internal DC stage (blue), and outputs AC at a variable frequency (orange). (a) A rectifier is required to convert 60 Hz AC (red) to DC. (b) A proposed modification, with multiplexed AC and DC inputs.

This work further classifies loads based on how they can benefit from an interface to a DC distribution network. In Fig. 1, common plug loads are classified as being:

- DC-connected: The internal DC stage of these loads can be connected or hardwired directly to the DC network. A direct-DC input would bypass the input voltage conversion (and/or rectification) stage. DC benefits these loads the most.
- DC-converted: The internal DC stage of these loads requires a DC/DC converter in order to connect to the DC network. However the direct-DC version often outperforms its native-DC counterpart. DC offers some benefits for these loads.
- DC-indifferent: The load can be hardwired to an AC or DC distribution with equivalent cost and efficiency. DC does not directly benefit these loads.

1) *DC-connected*: Includes loads with a fixed internal DC bus, many of which require AC power at a non-mains frequency.

VFD motor loads contain a brushless DC (BLDC) inverter-driven synchronous or asynchronous motor. Due to their efficiency benefits, VFDs will eventually replace fixed-speed motors in HVAC, refrigeration, and water heating. As shown in Fig. 2a, native-DC VFD motors require a rectification stage, followed by a DC capacitor bus. The inverter supplies the stator coils with a variable-frequency AC drive. In well-designed direct-DC VFDs, the DC capacitor bus could be connected directly to the DC distribution, as shown in Fig. 2b. A direct connection bypasses the rectification stage, thus allowing for savings in efficiency and cost. In addition, the DC bus capacitors can be reduced, as described in Appendix B.

Wireless transmitters power an antenna with high-frequency AC, and are structurally similar to VFDs: they

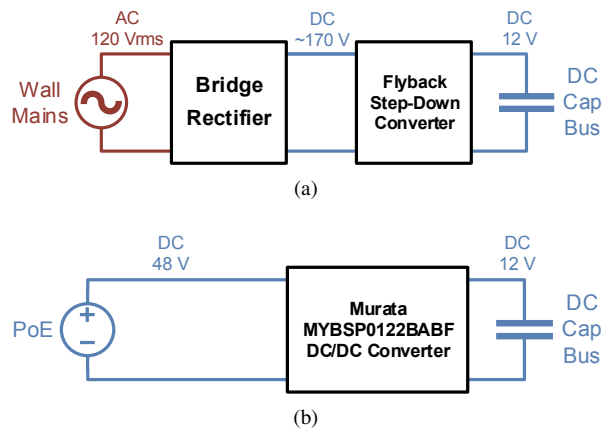


Fig. 3: Methods of providing power to the bath fan’s DC capacitor bus and inverter stages. (a) The fan’s original AC/DC rectifier board, shown in Fig. 5. (b) The DC-converted modification for 48 V PoE input, using a DC/DC converter.

contain a rectifier, DC bus, and power amplifier. Transmitters are present in any wirelessly connected electronics. Wireless chargers and induction stoves employ near-field wireless power transfer.

2) *DC-converted*: Includes current-controlled loads and loads with multiple internal voltage rails.

LEDs are a current-controlled load since their luminosity is nearly proportional to their current. DC LED drivers are often 95-98% efficient, whereas AC LED drivers commonly have 86-93% efficiency [7], [10]. In addition, AC LED drivers are more expensive because they have to rectify the AC input, apply power factor correction (PFC), and cancel the 120 Hz AC power ripple with a large electrolytic capacitor.

Laptops require several DC/DC converters to power the internal components at their respective voltages. Nonetheless, an AC/DC wall adapter is also required to supply the laptop’s primary power rail. DC input to the primary rail could obviate the need for a wall adapter, allowing for benefits similar to DC-connected devices.

3) *DC-indifferent*: Includes heating elements and fixed-speed motors. Resistive heating elements are often found in water heaters, ovens, and incandescent bulbs. These devices can be connected to AC or DC distributions with equal efficiency. Fixed-speed motors are often found in old or inexpensive motor loads. Due to their low efficiency in many applications, they will eventually be replaced by VFDs.

III. BATH FAN

A. Modifications for DC Input

There are two proposed modifications to the Delta GBR80 BLDC motor bath fan. The 48 V DC-converted modification in Fig. 3b is intended for PoE, and a 12 V DC-connected modification is for USB-C. Although PoE requires a 48/12 V DC/DC conversion, it is practical due to the distance limitations of USB-C. These modifications both maintain the DC bus at its nominal 12 V, since increasing or decreasing the bus voltage may damage the inverter or stator coils, respectively.

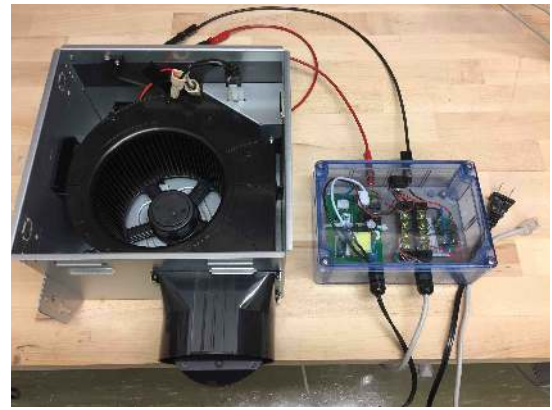


Fig. 4: Prototype of the Delta GBR80 bath fan, modified to accept a PoE input. The blue box contains the AC and DC input boards, with a switch to toggle between them.

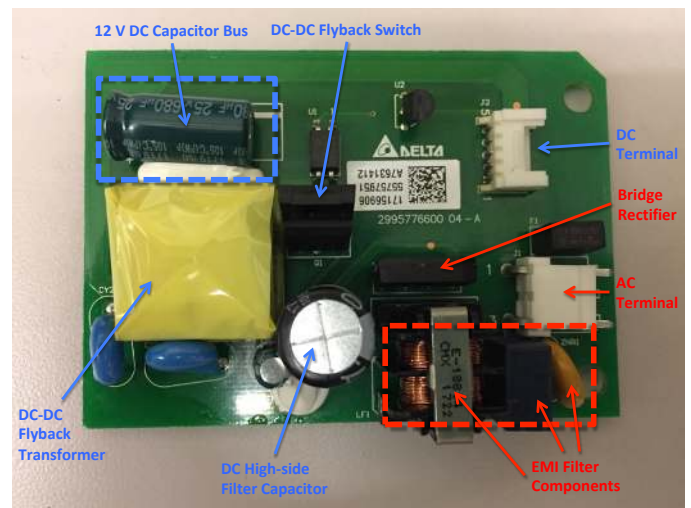


Fig. 5: The original rectifier board that converts 120 V_{RMS} AC to 12 V DC. The board dimensions are 8 x 6 cm.

As such, this experiment does not affect the motor’s speed and torque.

B. Experimental Prototype and Results

As shown in Fig. 4, the bath fan prototype has a multiplexed AC or DC input. The original rectifier board in Fig. 5 uses an isolated flyback topology. The DC-converted input uses the Murata MYBSP0122BABF isolated 48/12 V DC/DC converter.

The results suggest that direct-DC can improve the fan’s power consumption. The efficiency curves in Fig. 6 show that the DC/DC converter is up to 6% more efficient than the original rectifier board. Tab. I shows a decrease in the fan’s input power with DC input. In addition, the fan draws even less power with a 12 V input, which represents the savings potential of a DC-connected design. In this experiment, the exhaust valve is held open or shut to simulate a lightly or heavily loaded fan, respectively.

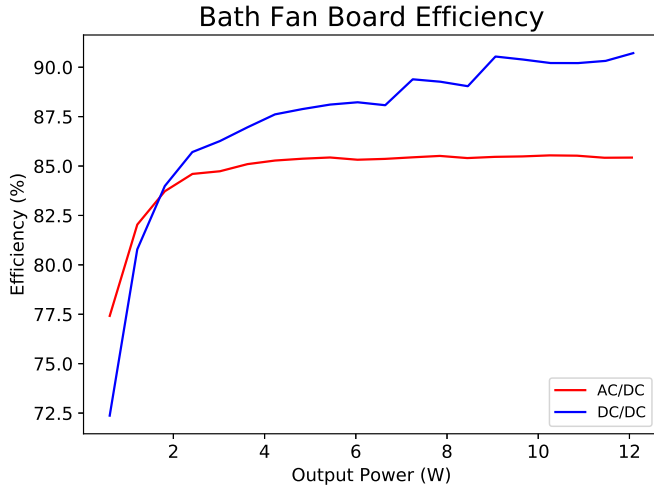


Fig. 6: Efficiency curves for the prototype bath fan’s AC/DC and DC/DC boards.

TABLE I: Fan prototype power consumption

Input Type	Conversion	Input Power Light Load	Input Power Heavy Load
120 V _{RMS} AC	AC/DC	7.75 W	9.01 W
48 V DC	DC/DC	7.43 W	8.65 W
12 V DC	None	6.6 W	7.72 W

C. Discussion

The 48 V DC-converted modification improves on the efficiency by removing the AC/DC rectification stage and allowing for a smaller DC/DC conversion ratio V_{out}/V_{in} . Although the 12 V DC-connected modification has the lowest cost and consumption, it is impractical for a bath fan due to low-voltage wire loss. Nonetheless, the 12 V modification is explicitly intended to show the benefits of a DC-connected design. Ideally, a PoE bath fan would have a 48 V inverter and motor. Appendix A shows how a BLDC motor can be redesigned to operate with a different internal DC voltage.

IV. REFRIGERATOR

A. Modifications for DC Input

The 11 ft³ LG LTNC11121V inverter-based refrigerator is modified for a DC-connected input by removing the Delon (full wave) doubler rectification stage, as shown in Fig. 7. Its nominal 340 V DC bus approximates the efficiency and power draw from 380 V DC distribution.

B. Experimental Prototype and Results

The refrigerator prototype, shown in Fig. 8, adds a 340 V DC-connected input to the DC capacitor stage. As shown in Fig. 9 the inverter board’s original AC input contains an input EMI filter and protection components. The efficiency of the rectification stage in Fig. 7a is 99%, averaged over fifty

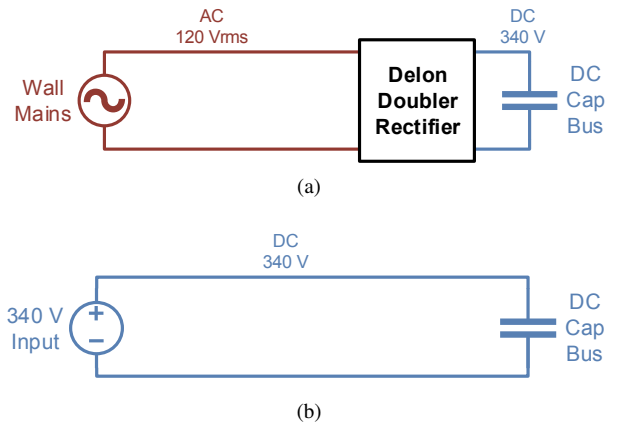


Fig. 7: Methods of providing power to the refrigerator’s DC capacitor bus and inverter stages. (a) The refrigerator’s original AC/DC Delon doubler rectifier circuit. (b) The DC-connected modification for 340 V input, which approximately represents 380 V DC.



Fig. 8: Prototype for the DC input modification of a refrigerator. The blue box on the left side allows for a 340 V DC input to the inverter board’s DC capacitor bus. The compressor is the BMA069LAMV model.

measurements with power ranging from 50 W to 80 W. The AC power factor is 0.65, and is caused entirely by harmonic distortion.

C. Discussion

The refrigerator barely benefits from a high-voltage DC input, since bypassing the rectification stage only saves 1% of the input power. 340 V operation can be very efficient, but requires the large inverter and capacitors shown in Fig. 9. In contrast, many low-voltage DC refrigerators can operate with smaller electronics, such as the 24 V Danfoss 101N0212. Compared to the LTNC11121V, its compressor has fewer and thicker windings, as discussed in Appendix A.

It is important to note that the LNTC11121V has a poor power factor of 0.65 due to its lack of power factor correction (PFC). This refrigerator barely falls under the threshold of mandatory PFC, as per the IEC 61000-3-2 Class D harmonic specifications [28]. Standard-sized refrigerators require a PFC

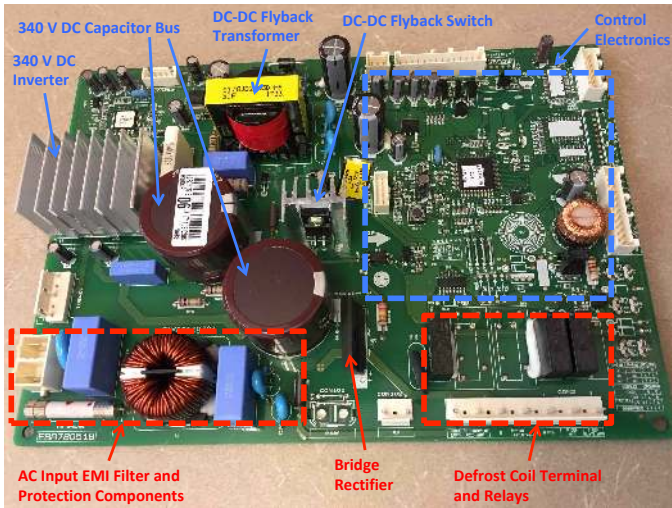


Fig. 9: Inverter board for the LG LTNC11121V refrigerator. The inverter is a high-voltage 3-phase SIM6822M chip. The board dimensions are 23 x 16 cm.

rectifier whose losses and cost are more substantial, and would benefit much more from a DC-connected input.

DC input allows for a reduction in the size of the DC capacitor bus. Not only are the high-voltage high-capacitance electrolytics in Fig. 9 bulky and expensive, but they are also prone to failure and may limit the life span of the entire board [29]. Appendix B describes how the giant DC capacitors in Fig. 9 are needed for filtering the 120 Hz AC power ripple, and can be greatly reduced with direct-DC.

V. TASK LIGHT

A. Modifications for DC Input

Task lights in a workspace can benefit from localized low-voltage DC distribution. Many USB task lights in today’s market are powered by a 5 V USB-A port and use a ballast resistor for current control. The ballast resistor makes the lamp inefficient, susceptible to input voltage swing, and difficult to dim. Advanced task lights overcome these difficulties with an LED driver. Future lamps may be powered by a USB-C charging station, as shown in Fig. 10a.

A further improvement is possible, shown in Fig. 10b, in which the charging station becomes the LED driver. This solution requires a charging station that supports USB protocols with a programmable power supply (PPS) capability (USB-PD 3.0 or QC 3.0). These lamps need only to sense the LED current and program the supply voltage accordingly. This method effectively removes the LED driver conversion stage, while still offering all its benefits.

B. Experimental Prototype and Results

The task light prototype demonstrates the driverless topology in Fig. 10b. It connects to an Anker PowerPort charger with QC 3.0 (USB-PD 3.0 was not available during this experiment). The Anker PowerPort provides up to 12 V to three 1.5 A LEDs (Cree MTG7-001I-XTE00-NW-0GE3). At

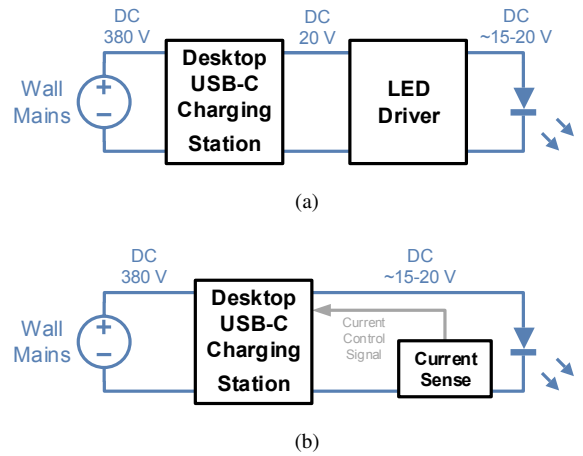


Fig. 10: Methods of powering a task lamp with DC input from a desktop charging station. Note that the wall mains could also be 120 V_{RMS} AC or 48 V DC. (a) Connect the LED driver in the lamp to the charging station’s output. (b) If the charging station has PPS capability, the charging station can become the constant current LED driver.

the brightest operating point, the LED string draws 1.5 A at 14.3 W (9.815 V). An Arduino microcontroller generates the brightness control signals, which are sent via the USB data lines as per the QC protocol. Although this proof-of-concept prototype uses voltage control, current control is generally recommended to account for temperature effects and such.

C. Discussion

The prototype effectively uses the charging station as an LED driver, thus reducing the number of power conversions. This method is possible in any point-to-point DC topology that supports a protocol with PPS capability.

VI. ZONE LIGHTING

A. Modifications for DC Input

Traditional LED bulbs have internal drivers, and are designed to plug into existing incandescent or fluorescent fixtures. As shown in Fig. 11a, the LED drivers are distributed between the fixtures and may require a separate signaling line for dimming. Although internal LED drivers are standard in AC buildings, they are also present in many of the experimental 380 V DC test beds [9], [10].

External or remote LED drivers are physically separate from the lamp’s LEDs. Several companies have started promoting their use in building lighting systems. First, remote drivers reduce component cost since each driver can power several fixtures. Second, easily accessible and replaceable remote drivers reduce maintenance costs, since the driver often limits the lifespan of the entire lamp. Finally, dimming and ancillary functions are more cost-effective with a centralized driver.

Most commercial remote LED drivers use a parallel design, which is ideal for applications that require individual fixture control. This work aims to demonstrate that a series topology,

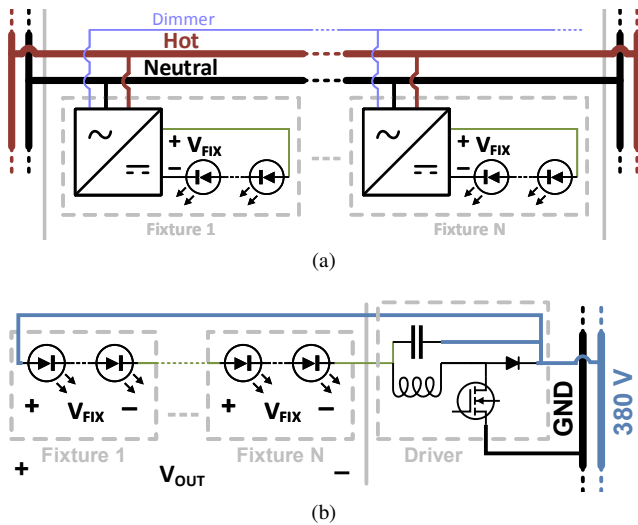


Fig. 11: Methods of wiring lighting fixtures. (a) The conventional design with distributed drivers and a dedicated 0-10 V analog dimming line. (b) Series-remote driver topology with a 380 V DC buck-based driver.



Fig. 12: Prototype of the series-remote driver zone light.

shown in Fig. 11b, is an excellent design for zone lighting in 380 V DC buildings. The cost benefit of the series-remote driver is in using simple low-power hardware to drive many fixtures. The efficiency benefit is in stacking LED fixtures to closely match 380 V.

B. Experimental Prototype and Results

A 380 V DC series-remote driver was prototyped using the buck-based topology in Fig. 11b. The prototype, shown in Fig.12, uses an MP4000 controller, a 600 V IGBT, and a 10 mH inductor. The experimental fixtures are a set of 75 V 18 W four-foot T8 LED tubes, which come from removing the driver of a PT-T84FP18W. As shown in Fig. 13, the driver's efficiency increases with the number of tubes. For reference, the original tube-integrated AC LED driver operates at 92% efficiency and 0.97 power factor.

C. Discussion

Remote drivers have many advantages over conventional internal drivers, such as cost, maintenance, and control func-

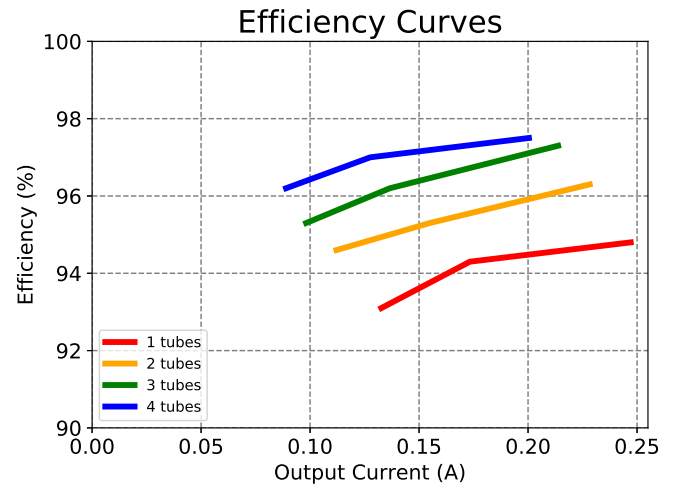


Fig. 13: Efficiency curves for the 380 V DC series-remote driver with 1-4 LED tubes attached in series. The driver's efficiency increases with the number of attached tubes.

tionality. However, the drawbacks are a loss of plug-and-play simplicity and possible voltage drop over long wire runs. Series-remote drivers add the potential to further improve on hardware costs and efficiency. Nonetheless, their drawbacks include non-trivial wiring and the inability to dim individual fixtures. As such, series-remote drivers are best suited for commercial zone lighting, and further study is required to fully determine their value in buildings.

One potential concern with series fixtures is that a single LED failure would disable the entire multi-fixture string. This drawback can be overcome by equipping each fixture with a bypass circuit. The simplest bypass circuit can be built from an SCR and a Zener diode [30].

Although the prototype only allows five 18 W 75 V tubes to be stacked in series, newer high-brightness LEDs provide more power with less voltage drop. For example, an 18 W bulb with three modern 6 V 1 A LEDs would only drop 18 V. Twenty-one such bulbs would stack to 380 V, which is enough to cover a moderately sized room. A buck-boost series-remote driver allows the flexibility of even more bulbs at the incremental cost of efficiency and safety.

VII. CONCLUSION

Buildings with DC power have taken the recent spotlight in research, but the development of highly efficient DC-ready loads has lagged. This work categorizes the types of loads whose efficiency directly benefits from a DC input. Several types of loads are studied, and some of them are modified or prototyped as direct-DC. This work focuses on low-power residential and small commercial loads, which include a bath fan, refrigerator, task lamp, and zone lighting system. The purpose of each design is to leverage DC input to eliminate or improve the conversion stages.

This project obtained new insights specific to the categories of motor loads, electronics, and lighting. In motor loads, the most efficient type of BLDC motor is designed such that its

internal DC capacitor bus is coupled to the DC input. Although there is very little loss across a diode bridge rectifier, a PFC boost rectifier is notably less efficient. In lighting, DC task lamps can leverage a USB-PD charging station as an LED driver. Zone lighting can benefit greatly from series-remote drivers, but further research must validate their feasibility. In all loads, DC input will improve power quality and reduce the size of the DC capacitors. Further study is required to determine the full value of these secondary effects.

APPENDIX

A. DC Capacitor Voltage in BLDC Motors

Brushless DC (BLDC) motors are designed with a specific AC voltage across the stator windings. The winding voltage dictates the inverter's DC capacitor bus voltage, which can be DC-connected if it equals the DC distribution voltage. This section shows how a motor's winding voltage can be designed independently of its power rating, and can ultimately be designed as a DC-connected device.

For a given application, assume the motor's electrical input power P_{const} is specified and constant, and its magnetic flux ϕ_{const} is constant and is directly related to the mechanical output power. The relations between the electrical stator windings and the magnetic core are:

$$P_{const} = VI \quad (1)$$

$$\phi_{const} = \frac{NI}{\mathcal{R}_{tot}} \quad (2)$$

$$E = N \frac{d\phi_{const}}{dt}, \quad (3)$$

where V and I respectively are the winding's input voltage and current, N is the number of windings, \mathcal{R}_{tot} is the total reluctance of the magnetic core, and E is the back EMF generated in the windings.

Consider two motors with the same power $P_1 = P_2$ and magnetic flux $\phi_1 = \phi_2$, but winding voltage $V_1 = KV_2$. Eq. 1 requires that $I_1 = \frac{1}{K}I_2$, and from Eq. 2 it follows that $N_1 = KN_2$. In other words, the motor 1 requires K times as many windings, but the windings only pass $\frac{1}{K}$ times as much current. As such, the overall winding packing window is roughly equal. Finally, Eq. 3 causes $E_1 = KE_2$, but since $V_1 = KV_2$, each motor can attain the same maximum speed.

The core loss is equal between the motors because $\phi_1 = \phi_2$. The winding loss is also equal, since the factor K falls out of the equations:

$$P_w = I^2 R_w = I^2 \rho \frac{L}{A}. \quad (4)$$

The wire loss P_w and resistance R_w are dependent on the wire length L , cross sectional area A , and resistivity ρ .

B. Sizing the DC Capacitor Bus

Most types of native-DC loads contain an internal DC capacitor bus, whose size can often be reduced in converting to a direct-DC input. These capacitors are sized such that the peak-to-peak bus voltage ripple, ΔV_C , is within specification. In native-DC loads, the DC capacitor bus is required for:

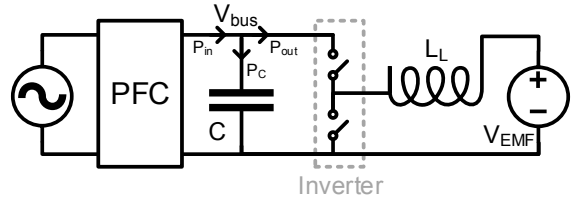


Fig. 14: A model of the energy flow in a VFD motor with PFC. The DC capacitor is responsible for absorbing the AC component of P_{in} , allowing for a purely DC P_{out} . In this model, the inverter is a half-bridge and the motor is represented by its winding inductance L_L and a constant back EMF.

- Filtering the 120 Hz power ripple from the AC input
- Filtering the inverter PWM current
- Providing an energy buffer for a change in load

In direct-DC loads, the DC capacitor bus is only responsible for the latter two. This section explains how to analytically determine the requisite capacitance C for VFD motor loads. It is based on the half-bridge inverter model in Fig. 14.

The DC bus ripple ΔV_C due to an AC input with unity power factor can be solved by an energy analysis [31]:

$$\Delta V_C = \frac{P_{in,avg}}{V_{DC}\omega_0 C}, \quad (5)$$

where V_{DC} is the DC bus voltage, $P_{in,avg}$ is the average input power, and $\omega_0 = 2\pi 60$. The maximum DC bus ripple due to inverter switching current harmonics is [32]:

$$\Delta V_C = \frac{V_{DC}}{32L_L C f^2}, \quad (6)$$

where L_L is the load or winding inductance. The bus capacitance required to provide an energy buffer for load transients is derived via a simple LC circuit. In this model, the inductor L_S represents the line inductance between the building's source and the motor load. When the motor circuit is subject to a transient current step of size M , the DC bus ripple is:

$$\Delta V_C = 2M \sqrt{\frac{L_S}{C}}. \quad (7)$$

The step response magnitude varies with application. Many of the VFD loads in Fig. 1 have nearly constant power draw, and transients only arise at start-up. VFD inverters can soft-start the motor, allowing for a start-up current that is always lower than the full-load current ($M = I_{out,max}$).

The design example uses the LG inverter refrigerator. As discussed in Section IV, the refrigerator draws as much as $P_{in} = 80$ W from a standard 60 Hz AC distribution. The inverter operates at $f = 20$ kHz, and is powered from a DC bus at $V_{DC} = 340$ V. In addition, the compressor's load inductance is dominated by a load-side reactor with $L_L = 0.8$ mH.

As shown in Table II, the DC bus voltage ripple ΔV caused by the AC input is considerably greater than the other two sources. With direct-DC input, the DC capacitors can be reduced a factor of ten to twenty. Applications with high input power P_{in} or low bus voltage V_{DC} are especially favorable with direct-DC.

TABLE II: DC bus voltage ripple due to each effect

C (uF)	AC Ripple (V)	PWM Ripple (V)	Transient Ripple (V)
10.0	78.02	3.32	0.82
100.0	7.8	0.33	0.26
1000.0	0.78	0.03	0.08

ACKNOWLEDGEMENTS

This work was supported by the California Energy Commissions EPIC Project EPC-15-024. The authors would like to thank Alan Meier, Leo Rainer, Bruce Nordman, Wei Feng, Chris Marnay, Vagelis Vossos, and Seth Sanders for their technical advice and support.

REFERENCES

- [1] S. Backhaus, G. W. Swift, S. Chatzivasilieiadis, W. Tschudi, S. Glover, M. Starke, J. Wang, M. Yue, and D. Hammerstrom, "DC Microgrids Scoping Study Estimate of Technical and Economic Benefits," Tech. Rep. LAUR1522097, Los Alamos National Laboratory, Mar. 2015.
- [2] P. Savage, R. R. Nordhaus, and S. P. Jamieson, "From Silos to Systems: Issues in Clean Energy and Climate Change: DC microgrids: benefits and barriers," tech. rep., Yale School of Forestry & Environmental Sciences, 2010.
- [3] V. Vossos, K. Garbesi, and H. Shen, "Energy savings from direct-DC in U.S. residential buildings," *Energy and Buildings*, vol. 68, Part A, pp. 223–231, Jan. 2014.
- [4] B. Glasgo, I. L. Azevedo, and C. Hendrickson, "How much electricity can we save by using direct current circuits in homes? Understanding the potential for electricity savings and assessing feasibility of a transition towards DC powered buildings," *Applied Energy*, vol. 180, pp. 66–75, Oct. 2016.
- [5] M. Noritake, K. Yuasa, T. Takeda, H. Hoshi, and K. Hirose, "Demonstrative research on DC microgrids for office buildings," in *Telecommunications Energy Conference (INTELEC), 2014 IEEE 36th International*, pp. 1–5, Sept. 2014.
- [6] S. Willems and W. Aerts, *Study and Simulation Of A DC Micro Grid With Focus on Efficiency, Use of Materials and Economic Constraints*. PhD thesis, University of Leuven, Leuven, Belgium, 2014.
- [7] D. L. Gerber, V. Vossos, W. Feng, C. Marnay, B. Nordman, and R. Brown, "A simulation-based efficiency comparison of ac and dc power distribution networks in commercial buildings," *Applied Energy*, vol. 210, pp. 1167 – 1187, 2018.
- [8] S. M. Frank and S. Rebennack, "Optimal design of mixed ac-dc distribution systems for commercial buildings: A nonconvex generalized benders decomposition approach," *European Journal of Operational Research*, vol. 242, no. 3, pp. 710 – 729, 2015.
- [9] U. Boeke and M. Wendt, "DC power grids for buildings," in *2015 IEEE First International Conference on DC Microgrids (ICDCM)*, pp. 210–214, June 2015.
- [10] D. Fregosi, S. Ravula, D. Brhlik, J. Saussele, S. Frank, E. Bonnema, J. Scheib, and E. Wilson, "A comparative study of DC and AC microgrids in commercial buildings across different climates and operating profiles," in *2015 IEEE First International Conference on DC Microgrids (ICDCM)*, pp. 159–164, June 2015.
- [11] G. AllLee and W. Tschudi, "Edison Redux: 380 Vdc Brings Reliability and Efficiency to Sustainable Data Centers," *IEEE Power and Energy Magazine*, vol. 10, pp. 50–59, Nov. 2012.
- [12] M. Wright, "Eaton demonstrates distributed DC power for LED lighting at LFI," *LEDs Magazine*, May 2016.
- [13] H. Kakigano, Y. Miura, and T. Ise, "Low-voltage bipolar-type dc microgrid for super high quality distribution," *IEEE Transactions on Power Electronics*, vol. 25, pp. 3066–3075, Dec 2010.
- [14] Y. Ito, Y. Zhongqing, and H. Akagi, "Dc microgrid based distribution power generation system," in *The 4th International Power Electronics and Motion Control Conference, 2004. IPEMC 2004.*, vol. 3, pp. 1740–1745 Vol.3, Aug 2004.
- [15] V. Vossos, S. Pantano, R. Heard, and R. Brown, "Dc appliances and dc power distribution," 2017.
- [16] A. Mishra, K. Rajeev, and V. Garg, "Assessment of 48 volts dc for homes," in *2018 IEEMA Engineer Infinite Conference (eTechNxT)*, pp. 1–6, IEEE, 2018.
- [17] M.-H. Ryu, H.-S. Kim, J.-W. Baek, H.-G. Kim, and J.-H. Jung, "Effective test bed of 380-v dc distribution system using isolated power converters," *IEEE transactions on industrial electronics*, vol. 62, no. 7, pp. 4525–4536, 2015.
- [18] G. Makarabbi, V. Gavade, R. Panguloori, and P. Mishra, "Compatibility and performance study of home appliances in a dc home distribution system," in *Power Electronics, Drives and Energy Systems (PEDES), 2014 IEEE International Conference on*, pp. 1–6, IEEE, 2014.
- [19] M. Noritake, K. Yuasa, T. Takeda, K. Shimomachi, R. Hara, H. Kita, and T. Matsumura, "Experimental study of a 400 v class dc microgrid for commercial buildings," in *Power Electronics and ECCE Asia (ICPE-ECCE Asia), 2015 9th International Conference on*, pp. 1730–1735, IEEE, 2015.
- [20] A. Stippich, A. Sewergin, G. Engelmann, J. Gottschlich, M. Neubert, C. van der Broeck, P. Schuelting, R. Goldbeck, and R. De Doncker, "From ac to dc: Benefits in household appliances," in *International ETG Congress 2017; Proceedings of*, pp. 1–6, VDE, 2017.
- [21] A. Jhunjhunwala, K. Vasudevan, P. Kaur, B. Ramamurthi, S. Bitra, K. Uppal, et al., "Energy efficiency in lighting: Ac vs dc led lights," in *Sustainable Green Buildings and Communities (SGBC), International Conference on*, pp. 1–4, IEEE, 2016.
- [22] M. G. Jahromi, G. Mirzaeva, S. D. Mitchell, and D. Gay, "Dc power vs ac power for mobile mining equipment," in *Industry Applications Society Annual Meeting, 2014 IEEE*, pp. 1–8, IEEE, 2014.
- [23] D. Das, N. Kumaresan, V. Nayanar, K. N. Sam, and N. A. Gounden, "Development of bldc motor-based elevator system suitable for dc microgrid," *IEEE/ASME Transactions on Mechatronics*, vol. 21, no. 3, pp. 1552–1560, 2016.
- [24] K. Yukita, T. Hosoe, S. Horie, T. Matsumura, M. Hamanaka, K. Hirose, and M. Noritake, "Air conditioning equipment using dc power supply system," in *Telecommunications Energy Conference (INTELEC), 2017 IEEE International*, pp. 229–232, IEEE, 2017.
- [25] P. Rani, D. Vignesh, S. Gunaki, and A. Jhunjhunwala, "Design of converters for leveraging 48v dc power line at homes/offices," in *Sustainable Green Buildings and Communities (SGBC), International Conference on*, pp. 1–5, IEEE, 2016.
- [26] O. Lucia, I. Cvetkovic, H. Sarnago, D. Boroyevich, P. Mattavelli, and F. C. Lee, "Design of home appliances for a dc-based nanogrid system: An induction range study case," *IEEE Journal of Emerging and Selected Topics in Power Electronics*, vol. 1, no. 4, pp. 315–326, 2013.
- [27] OSHA 1910.303(g)(2)(i), "Guarding requirements for 50 volts or more DC," standard, Occupational Safety and Health Administration, Washington, D.C., 2015.
- [28] I. IEC, "61000-3-2: 2014 electromagnetic compatibility (emc)-part3-2: Limits-limits for harmonic current emissions (equipment input current 16a per phase)," *British Standards Institute*, 2014.
- [29] W. Chen and S. R. Hui, "Elimination of an electrolytic capacitor in ac/dc light-emitting diode (led) driver with high input power factor and constant output current," *IEEE Transactions on Power Electronics*, vol. 27, no. 3, pp. 1598–1607, 2012.
- [30] K. Bollmann and T. C. Penick, "Led lighting system with bypass circuit for failed led," Apr. 2 2013. US Patent 8,410,705.
- [31] D. L. Gerber, C. Le, M. Kline, S. Sanders, and P. Kinget, "An integrated multilevel converter with sigma-delta control for led lighting," *IEEE Transactions on Power Electronics*, pp. 1–1, 2018.
- [32] M. Salcone and J. Bond, "Selecting film bus link capacitors for high performance inverter applications," in *Electric Machines and Drives Conference, 2009. IEMDC'09. IEEE International*, pp. 1692–1699, IEEE, 2009.